Helix-like structure formation of a semi-flexible chain confined in a cylinder channel*

Xiaohui Wen(温晓会)[1,2,†], Tieyu Sun(孙铁昱)[2], Wei-Bing Zhang(张卫兵)[3], Chi-Hang Lam(林志恒)[2], Linxi Zhang(章林溪)[4], and Huaping Zang(臧华平)[5]

[1] *Department of Applied Physics, Chengdu University of Technology, Chengdu* 610059, *China*
[2] *Department of Applied Physics, The Hong Kong Polytechnic University, Hong Kong SAR, China*
[3] *School of Physics and Electronic Sciences, Changsha University of Science and Technology, Changsha* 410004, *China*
[4] *Department of Physics, Zhejiang University, Hangzhou* 310027, *China*
[5] *School of Physics and Engineering, Zhengzhou University, Zhengzhou* 450002, *China*

(Received 21 February 2016; revised manuscript received 25 April 2016; published online 20 July 2016)

Molecular dynamics method is used to study the conformation behavior of a semi-flexible polymer chain confined in a cylinder channel. A novel helix-like structure is found to form during the simulation. Moreover, the detailed characteristic parameters and formation probability of these helix-like structures under moderate conditions are investigated. We find that the structure is not a perfect helix, but a bundle of elliptical turns. In addition, we conduct a statistical analysis for the chain monomer distribution along the radial direction. This research contributes to our understanding of the microscopic conformation of polymer chains in confined environments filled with a solvent.

Keywords: semi-flexible polymer, cylinder channel, solvent, helix-like structure

PACS: 36.20.Ey, 87.15.A–, 87.15.ap, 02.50.–r **DOI:** 10.1088/1674-1056/25/9/093601

1. Introduction

Conformation transition of a semi-flexible polymer chain in a confined environment is ubiquitous in nature and has a variety of physical and biological applications. As a representative example, biological macromolecules such as DNA, RNA, and proteins, which are known to be confined in cells, have attracted more and more researchers' attention.[1–7] A single DNA chain has a persistence length of approximately 50 nm, but it can be folded in a small cell with a diameter at only several micrometres. To understand the conformation of macromolecules in confined environments, a considerable number of studies have been conducted involving experiments,[8–14] theories,[15–22] and simulations.[2–7,17,23–34] For instance, Reisner *et al.* experimentally studied the physics and biological applications of DNA confined in nanochannels,[13] and found that these fascinating systems can be used to probe single-molecule conformation in environments with key physical length-scales ranging from 1 nm to 100 μm. Theoretically, Tree *et al.* suggested that the extension of DNA in a nanochannel is a Rod-to-Coil transition,[22] and showed that there exists a universal, Gauss–de Gennes regime that connects the classic Odijk and de Gennes regimes of channel-confined chains, especially for DNA in a nanochannel. Lv *et al.* simulated the self-assembly of double helical nanostructures inside carbon nanotubes.[25] The computational results indicated that the SWNT size and the polymer chain stiffness determine the outcome of the nanostructure while water clusters encourage the self-assembly of polyamide (i.e., PA) helical structures in a tube.

Numerous studies mainly focus on the insertion of polymer chains into hollow cylinder channels in a vacuum. The solvent is typically omitted or replaced by a simple frictional force for simplicity. We expect that the presence of solvent molecules could significantly impact this dynamic. Since the solvents have important functions in physical, chemical, and particularly biochemical processes,[35] it is important to investigate their effects on the conformation and dynamics of polymers. In particular, solvents may assist the self-assembly of new biological nanostructures.

In this paper, we investigate the confined conformation and distribution behaviors of a semi-flexible linear polymer chain confined in a cylinder channel using molecular dynamics method. In order to simulate a realistic solution environment, the cylinder channel is filled with solvent particles. The conformation behaviors under various values of stiffness of the semi-flexible polymer chains and radius of the cylinder channels are examined in detail. This work may supply a theoretical foundation for the future theories of conformation prediction and material fabrication.

*Project supported by the National Natural Science Foundation of China (Grant Nos. 11504033 and 11404290) and the General Research Fund of Hong Kong Research Council of China (Grant No. 15301014).
†Corresponding author. E-mail: wenxiaohui_2006@126.com
© 2016 Chinese Physical Society and IOP Publishing Ltd

2. Model and simulation

Dahirel *et al.* have developed a new coarse-graining procedure for the dynamics of charged spherical nanoparticles in solutions,[36] which reasonably reproduces the dynamics of charged nanoparticles in suspensions. Additionally, Malevanets *et al.* have studied solute molecular dynamics in a mesoscale solvent.[37] They developed a hybrid molecular dynamics algorithm by combining a full molecular dynamics (MD) description of solute–solute and solute–solvent interactions with a mesoscale treatment of solvent–solvent interactions. Here, we describe the dynamics of polymer chain and solvent particles in MD method.

Our initial system comprises three parts: (i) a single linear polymer chain consisting of multiple monomers, which is the main interest of this research; (ii) solvent particles serving as a solution environment; (iii) a cylinder channel with a fixed radius formed by a regular array of particles, which represents the static confinement environment. The first two parts are confined in the third part. A periodical condition is applied in the axial direction of the cylinder (z-axis). In the simulation, reduced units are used for simplicity. The chain monomer, all of solvent particles, and the cylinder channel particles are set to with mass $m = 1$ and diameter $\sigma = 1$.

The bead–spring model is used to simulate the polymer chain, which comprises N monomers. The interactions between adjacent polymer monomers are described by the finitely extensible nonlinear elastic (FENE) potential

$$U_{\mathrm{FENE}}(r) = -\frac{KR_0^2}{2}\ln\left[1-\left(\frac{r}{R_0}\right)^2\right] + 4\varepsilon\left[\left(\frac{\sigma}{r}\right)^{12}-\left(\frac{\sigma}{r}\right)^{6}\right]+\varepsilon, \quad (1)$$

where r is the distance between the two monomers, K is the spring constant, R_0 is the maximum allowed separation between connected monomers, and ε is the strength of the potential. It should be noted that the bonded potential between adjacent monomers includes the Lennard–Jones (L–J) potential as shown in Eq. (1). Here we choose $K = 30\varepsilon/\sigma^2$, $R_0 = 1.5$, and $\varepsilon = 1$.

The non-bonded interactions between nonadjacent polymer monomers, solvent particles, polymer monomer and solvent particle, polymer monomer and cylinder channel particle, solvent particle and cylinder channel particle are described by the truncated and shifted L–J potential, which is used to avoid discontinuity of the potential

$$U_{\mathrm{LJ}}(r) = \begin{cases} 4\varepsilon\left[\left(\frac{\sigma}{r}\right)^{12}-\left(\frac{\sigma}{r}\right)^{6}\right]-4\varepsilon\left[\left(\frac{\sigma}{r_c}\right)^{12}-\left(\frac{\sigma}{r_c}\right)^{6}\right], \\ \quad \text{for } r < r_c, \\ 0, \quad \text{for } r \geq r_c. \end{cases} \quad (2)$$

For the polymer monomers, the cut-off distance of the non-bonded interaction is set to $r_c = 2.5\sigma$, which means that the interactions include both repulsive (when $r < 2^{1/6}\sigma$) and attractive ones (when $2^{1/6}\sigma \leq r < 2.5\sigma$). For interactions between other particles, the cut-off distance is $r_c = 2^{1/6}\sigma$, which means that the truncated L–J potential is exclusively repulsive.

Moreover, the linear polymer chain stiffness is simulated by the bending potential

$$U_{\mathrm{bend}}(\theta) = b(1+\cos\theta), \quad (3)$$

where θ represents the angle of subtended between any two consecutive bonds in the chain, and b denotes the bending energy parameter, which quantifies the chain. $b = 0$ indicates that the chain is flexible, $b > 0$ indicates that the chain is semi-flexible, and $b \to \infty$ indicates that the chain is a rigid aligned rod. In this study, we will mainly focus on semi-flexible polymer chains.

The number of monomer N in a polymer chain, which is also the chain length, is set to 50, 100, and 200. The bending parameter b is set to 0, 10, 20, 30, 40, 50, 60, 70, 80, 90, 100, 200, 300, 400, 500, 600, 700, 800, 900, and 1000. The density ρ of mobile particles, including monomers and solvent particles, is fixed at $0.85\sigma^{-3}$. The radii of cylinder channel are set to 3, 4, and 5, which are all in units of σ. Due to the excluded volume interactions between mobile particles and static cylinder channel particles, the effective radii of the channel actually are $R = 2$, 3, and 4. To clearly describe the confinement, we define a physical parameter $\gamma = N/(\pi R^2)$, which is the ratio of chain length and the cross-sectional area. Its physical meaning is the monomer number per unit area, the larger the value of γ is, the stronger the confinement is.

Nosé–Hoover thermostat[35] and velocity-Verlet algorithm[38] are used. The time unit is $\tau = \sigma(m/\varepsilon)^{1/2}$, and the time step is $\Delta t = 0.001\tau$. Each simulation is repeated 5 times to obtain statistically averaged results. All the simulations are conducted with the LAMMPS MD package.[38]

3. Result and discussion

3.1. Helix-like structure of the polymer chain

Under the confined environments formed by the cylinder channels and the solvent particles, the conformation behaviors of the polymer chains change considerably. Here we choose two samples to demonstrate the changes. Figure 1 shows two examples of the progress of helix formation with the same parameters $b = 80$ and radius $R = 3$, but with different chain length: $N = 100$ in Fig. 1(a) and $N = 200$ in Fig. 1(b), respectively. Here the cylinder channel particles are not shown for clarity. As shown in Fig. 1(a), the chain can be viewed as a random coil at $t = 10\tau$. It begins to writhe at one end at $t = 100\tau$. Half of the chain has formed a helix-like structure at $t = 400\tau$. Almost the whole chain writhes to form a helix-like



Fig. 1. (color online) Snapshots of two typical helix formation processes for confined polymer chains at various times. Both of them have the same chain stiffness parameter $b = 80$. The number of monomers (red) in each chain is $N = 100$ for (a) and $N = 200$ for (b), respectively. Here the cylinder channel is not shown for clarity and the solvent particles are represented by white dots.

structure at $t = 1420\tau$. At last, a helix-like structure is formed at $t = 1800\tau$. As shown in the snapshots, the formed helix structure exhibits a bundle of turns stuck together. This can be explained by the attractive interactions among monomers. For the cases of $N = 200$ in Fig. 1(b), the formation process of a helix-like structure is completely different. The chain is a random coil at $t = 10\tau$, similar to that of $N = 100$. However, there are two helix-like rounds formed from its two ends at $t = 200\tau$. In the following time steps, the two helices approach, touch, collide and separate repeatedly till $t = 6800\tau$. At $t = 9400\tau$, the two coils have already overlapped with each other. At $t = 15800\tau$, the two coils have merged and a helix-like structure is formed. It is however not circular as reported previously,[25] but elliptical. This new helix-like structure is formed due to the cylinder channel's confinement effect as well as the exclusion effect of the solvent.

In order to quantitatively describe the helical periodicity, a spatial correlation function[39] is studied

$$G(s) = \frac{1}{N-3}\sum_{i=2}^{N-2} g(s,i). \tag{4}$$

Here, s is a sequence interval ranging from 0 to $N/2-1$ and $g(s,i)$ is given by[39]

$$g(s,i) = \frac{1/(N-s-1)\sum_{j=1}^{N-s-1}(\cos\beta_{i,j} - \langle\cos\beta_{i,j}\rangle)(\cos\beta_{i,j+s} - \langle\cos\beta_{i,j}\rangle)}{1/(N-1)\sum_{j=1}^{N-1}(\cos\beta_{i,j} - \langle\cos\beta_{i,j}\rangle)^2}. \tag{5}$$

The cosine of angle $\beta_{i,j}$ can be calculated with

$$\cos\beta_{i,j} = \frac{\boldsymbol{l}_i \cdot \boldsymbol{l}_j}{|\boldsymbol{l}_i||\boldsymbol{l}_j|}. \tag{6}$$

Here, $\boldsymbol{l}_i = \boldsymbol{r}_{i+1} - \boldsymbol{r}_i$ is the i-th bond vector, and $\langle\cos\beta_{i,j}\rangle$ denotes the average value of $\cos\beta_{i,j}$ over j from 1 to $N-1$.

$G(s)$ can be fitted with the empirical equation[39]

$$G(s) = \exp(-s/\xi)\cos(2\pi s/P). \tag{7}$$

Here, ξ and P denote the orientation correlation length and helix period, respectively. P represents the average number of monomer per turn in a polymer chain, and ξ describes the correlation of monomers along the chain contour. For a perfect helix, ξ tends to be infinite, while an exponential decay with no oscillations would be observed for non-periodical conformations.

For a polymer chain with chain length $N = 100$ confined in a cylinder with $R = 3$, the values of $G(s)$ are shown in Fig. 2(a), which provide further evidence for helical conformations of the confined chains with various b. For $b = 0$ and 1000, there are no periodical oscillations, which imply that they are not helix structures. When $b = 0$, an irregular coil is formed. When $b = 1000$, the chain is straight. When $b = 50$, 100, and 500, the curves show oscillations, which indicate that the chains have helix structures with three, two, and one helix turns, respectively. We obtain $\xi = 382$, $P = 34$; $\xi = 353$, $P = 54$ and $\xi = 480$, $P = 75$ by fitting to Eq. (7). Except for the ultra-soft and ultra-rigid chains, the stiffer the chain is, the fewer turns and the more monomers per turn it has.

Figure 2(b) illustrates various values of spatial correlation function under identical chain stiffness $b = 70$. From top to bottom, the three plots correspond to chain length $N = 50$, 100, and 200, respectively. Meanwhile, each plot has three curves, which show results for $R = 2$, 3, and 4. We find that the number of turns increases with the chain length. As all the plots have the same tendency, we take the middle plot for further discussions. By fitting the curves with Eq. (7), we obtain $\xi = 249$, $P = 54$; $\xi = 248$, $P = 43$ and $\xi = 1181$, $P = 35$ corresponding to $R = 2$, 3, and 4, respectively. We can see that the number of monomers per turn decreases with the effective radius. Usually, the opposite results are observed. Our results

here can be explained by the fact that the axis of the ellipsoidal helix chain is not parallel to the z-axis as shown in Fig. 3.

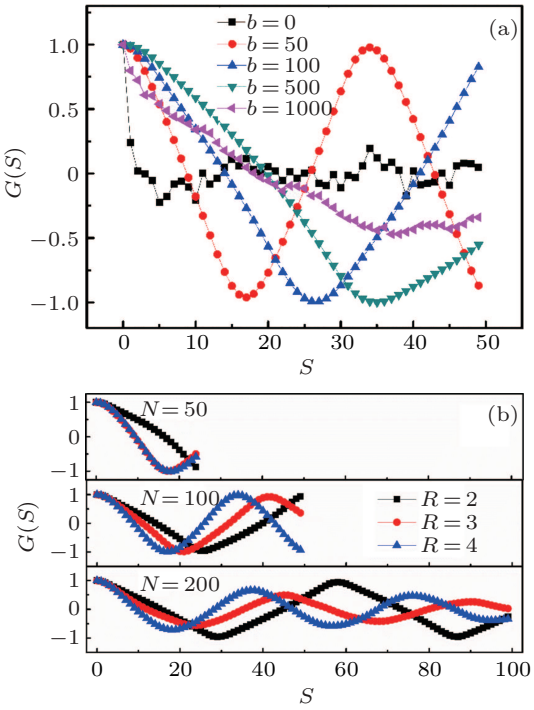


Fig. 2. (color online) Spatial correlation function $G(s)$ of confined polymer chains varies with sequential interval. (a) Results with radius $R = 3$ and $N = 100$.(b) Results with chain stiffness parameter $b = 70$ and chain length $N = 50$, 100, and 200, respectively. Each plot has three curves corresponding to channel radius $R = 2$, 3, and 4.

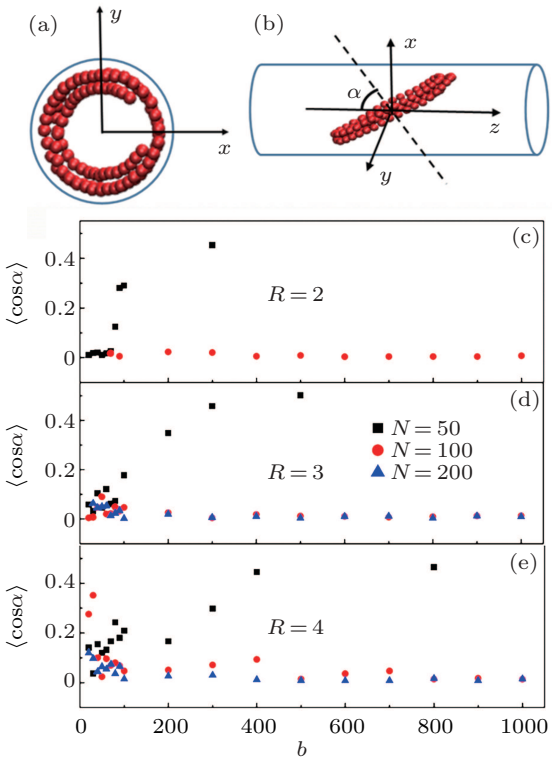


Fig. 3. (color online) (a), (b) The cross sections perpendicular and parallel to the cylinder channel, where α is the included angle between the normal direction of ellipsoid of the helix structure and the z-axis. (c)–(e) Variation of $\langle\cos(\alpha)\rangle$ with chain stiffness parameter b under different action radius $R = 2$, 3, and 4, where each has several curves for different chain monomer number N.

Figures 3(a) and 3(b) show a conformation as viewed from different angles. In particular, figure 3(b) shows that there is an angle α subtended between the axis of the helix and the z-axis. Figures 3(c)–3(e) show the average of $\cos\alpha$ for $R = 2$, 3, and 4, respectively. Figure 3(c) does not include the data for $N = 200$, because the channel is too thin for the long chain to form a helix structure. In addition, it should be noted that when $b = 0$ and 10, the chains exhibit random coils, so the values of $\langle\cos\alpha\rangle$ are non-plotted. The values of $\langle\cos\alpha\rangle$ for $N = 50$ are between 0 and 0.5, corresponding to the values of α between 90° and 30°. For $N = 200$, the values of $\langle\cos\alpha\rangle$ approach 0, indicating α approaching 90°. The reason is the emptying effect of the solvent particles, i.e., due to the attraction effect of chain monomers and the exclusive volume effect of solvent particles, the polymer chain adheres to the cylinder channel as much as possible. Therefore, with the same radius R, the inclination angle α is smaller than 90°, while that of a long chain is close to 90°. Figures 3(d) and 3(e) illustrate the values of $\langle\cos\alpha\rangle$ for $R = 3$ and 4. Each of them has three groups of data, and the characteristic is similar to that of Fig. 3(c). These results show that when $N = 50$, the values of $\langle\cos\alpha\rangle$ are larger than those of $N = 100$ and 200 with the axes of the ellipsoids perpendicular to the z-axis. We conclude that the axis of the ellipsoid is not along the z-axis.

In order to understand the number of turns of the chain intuitively, we plot the average bond angle $\langle\theta\rangle$ along a chain in Fig. 4(a). When a polymer chain with a length $N = 100$ is confined in a cylinder channel with radius $R = 3$, the five curves in Fig. 4(a) correspond to the five chain stiffnesses $b = 0$, 50, 100, 500, and 1000, respectively. As we know, for a perfect helix structure, the magnitude of average bond angle is almost equivalent, and the average bond angle is constant along the chain. However, figure 4(a) shows that each curve has several peaks, indicating that the cross sections of the helix structures are not circles but ellipses. When $b = 0$, the average bond angle $\langle\theta\rangle$ is around 1.75 radians, implying that the chain is a flexible coil. When $b = 50$, 100, and 500, the curves have five, three or two peaks, respectively. As we know, two peaks constitute one turn of an ellipsoidal helix structure. There are 2.5, 1.5, and 1 turns, respectively. When $b = 1000$, all the average bond angles nearly equal to 3.1, implying the chain is an aligned chain due to its large stiffness parameter. We can see that under a confined environment combined with solvent particles, a flexible chain or a rigid chain cannot form a helix structure, while a semi-flexible chain can form an elliptic helix structure.

Figure 4(b) shows the average bond angle $\langle\theta\rangle$ under a chain stiffness $b = 70$. Plots from the top to the bottom correspond to different chain lengths $N = 50$, 100, and 200, respectively. Each plot contains three curves corresponding to radius $R = 2$, 3, and 4, respectively. It is shown that the three plots

have the same tendency. We further discuss the middle plot, which has a chain length $N = 100$. There are 3, 4, and 5 peaks when $R = 2$, 3, and 4, respectively. We conclude that with a fixed chain stiffness b, the number of turns decreases with the radius.

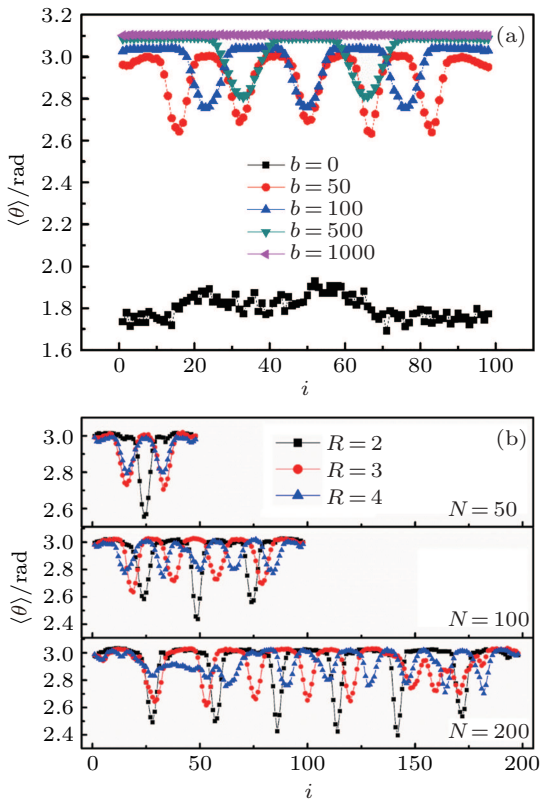


Fig. 4. (color online) (a) The bond angle $\langle\theta\rangle$ variation along a chain bond i with identical action radius $R = 3$ and chain monomer number $N = 100$, where five curves for different chain stiffness are illustrated for comparisons. (b) Results with identical chain stiffness parameter $b = 70$ and different monomer number $N = 50$, 100, and 200 from the top to the bottom. Each plot has three curves corresponding to the different cylinder radius $R = 2$, 3, and 4.

To determine the helical conformations in more details, the combination of $\cos(\phi_i)$ and $\cos(\varphi_i)$ is used, as shown in Fig. 5. As we know, the cylinder channel is periodical and the helix structure is along the z-axis. Therefore, we only discuss the helix structure projection of confined chain in the xy-plane. We define $\cos(\phi_i)$ and $\cos(\varphi_i)$ as

$$\cos(\phi_i) = \frac{\boldsymbol{b}_i \cdot \boldsymbol{b}_0}{|\boldsymbol{b}_i|}, \tag{8}$$

$$\cos(\varphi_i) = \frac{\boldsymbol{b}_i \cdot \boldsymbol{b}_1}{|\boldsymbol{b}_i||\boldsymbol{b}_1|}. \tag{9}$$

Here $\boldsymbol{b}_i = \boldsymbol{r}_{i+1} - \boldsymbol{r}_i$, where $\boldsymbol{r}_i = (x_i, y_i)$ is the projection of i-th bond vector in the xy-plane, and $\boldsymbol{b}_0 = (1, 0)$ is a constant vector.

For radius $R = 4$, figure 5(a) shows the results of $\cos(\phi_i)$ and $\cos(\varphi_i)$ with chain length $N = 100$ and chain stiffness $b = 200$. The two curves oscillate uniformly, which indicate both of them are helix structures. The periodic numbers of the uniform oscillation in the two curves correspond to the number of helix-like turns. Therefore, through calculations of $\cos(\phi_i)$ and $\cos(\varphi_i)$, the spatial correlation function $G(s)$ and average angle parameter $\langle\theta\rangle$ above, we can obtain the number of monomers per turn as well as the number of helix-like turns. Therefore, $\cos(\phi_i)$ and $\cos(\varphi_i)$ are other parameters to verify the helix-like structure. Here, the number of monomers per turn is 44 and the number of helix turns is 2.5.

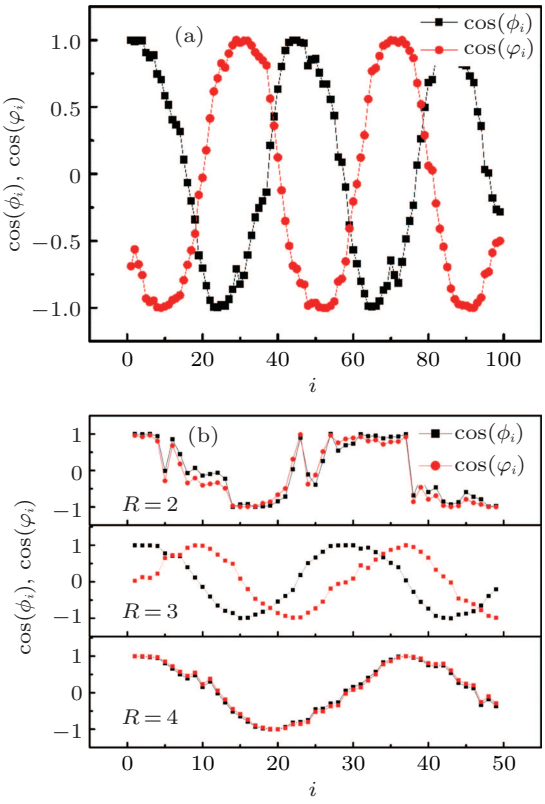


Fig. 5. (color online) (a) $\cos(\phi_i)$ and $\cos(\varphi_i)$ as a function of chain bond i for action radius $R = 3$, monomer number $N = 100$, and chain stiffness parameter $b = 200$. (b) Comparisons with identical chain monomer number $N = 50$ and chain stiffness parameter $b = 200$, but with different cylinder radius $R = 2$, 3, and 4 from the top to the bottom. Each plot has two curves corresponding to $\cos(\phi_i)$ and $\cos(\varphi_i)$, respectively.

In Fig. 5(b), with identical chain length $N = 50$ and chain stiffness $b = 200$, we compare the results of $\cos(\phi_i)$ and $\cos(\varphi_i)$ with different cylinder radius. When $R = 2$, there are no uniform oscillations in the two curves, which imply that the chain is a random coil. It is because the effective radius R is small, and the chain is compressed into a hank. Meanwhile for $R = 3$ and 4, the four curves are all of periodical uniform oscillation, and there are three and two peaks, respectively. The reason is that when the chains have identical length and stiffness, the thicker the channel is, the less turns the chain has to go around it. Here, the number of monomers per turn is 30 and 37 for $R = 3$ and 4, respectively. Correspondingly, with the same chain length, the number of turns of $R = 3$ is larger than that of $R = 4$.

We try to explain the reason of the helix-like formation by the entropy driving. Figures 6(a) and 6(b) represent the schematic diagrams of rod-like structure and helix structure, respectively. The excluded volume in Fig. 6(b) is generated by the polymer overlaps.[40] The change in free energy ΔF between the confined chains with helical structures and the confined chains with the rod-like structures can be written as $\Delta F = F_{\text{helix}} - F_{\text{rod-like}} = nk_{\text{B}}T\Delta V_{\text{overlap}} + \Delta U - T\Delta S$, where $\Delta V_{\text{overlap}}$ is the overlap volume of the excluded volume, ΔU is the change in the total energy, ΔS is the change in conformational entropy, and $n\Delta V_{\text{overlap}}$ is the total overlap volume of excluded volume.[41,42] The helical structure contributes to the increase of overlap volume. In Fig. 6(b), there is overlap of the excluded volume between the layers of the helix and in the central core region of the helix, and the excluded volume decreases by the overlap volume. Within moderate range of b, the effect of overlap volume is dominant, and the value of $nk_{\text{B}}T\Delta V_{\text{overlap}}$ is equal to or greater than that of $\Delta U - T\Delta S$, i.e., $\Delta F \leq 0$, when the polymer can form a helix structure. Previously, Magee *et al.*.[43] and Yang *et al.*.[29] have also demonstrated that delicate interplay between attractive interaction and packing (due to the excluded volume effect) of monomers could induce a helix structure, which supports our arguments.

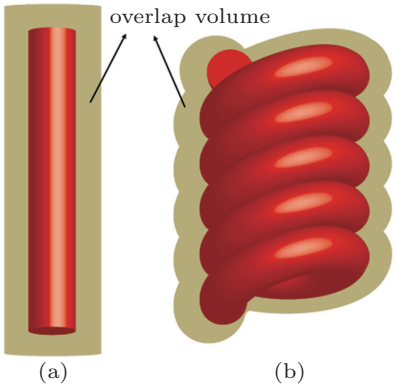


Fig. 6. (color online) Schematics of excluded volume (yellow) for the polymer chains, whose conformations are (a) rod-like and (b) helix structure.The excluded volume decreases by overlap when the confined semi-flexible chain forms a helix.

3.2. Distribution of chain monomer and helix-like formation percentage

We also study the distribution of the polymer chain monomers along the radial direction of the cylinder channel which are shown in Fig. 7. Here, the horizontal axis shows the radius of the cylinder, but not effective radius. Figure 7(a) shows the monomer distribution percentage P_0 along the radial direction of cylinder with various chain stiffness b, fixed effective radius $R = 3$, and chain length $N = 100$, when the radius of cylinder is 4.0 accurately. Firstly, we can see that the monomers accurately distribute at $r = 0 \sim 3.4$, most monomers locate at $r = 3.0$, but never distribute in the region of $r > 3.4$. The reason is that due to the exclude volume effect between the mobile particles and the static cylinder channel particles, their equilibrium distance is 1.0. Similar physical mechanism can be found in Fig. 7(b). When $b = 0$, the chain shrinks into itself and exhibits a coil, the percentages of the monomer distribution in the range of every average radius zone are all less than 15%. This is because of the flexible property of the polymer chain, the attraction effect of the L–J potential between non-bonded monomers as well as the exclude volume effect between the chain monomers, and the solvent particles affect the chain's conformation jointly. When $b = 50$, there are two peaks in the distribution curve located at $r = 2.0$ and $r = 3.0$, which correspond to $P_0 = 20\%$ and $P_0 = 50\%$, respectively. The reason is that, there are two adjacent turns along the radial direction, and the distance between every two adjacent turns is 1.0. The radial position of the turn clinging to the cylinder channel is $r = 3.0$, and the other turn's radial position is $r = 2.0$. From P_0 of the two turns, we can calculate the ratio of their monomer number to be 1:2.5. For $b = 100$, 500, and 1000, the monomers all cling to the cylinder channel wall, so their distribution curves have only one peak each, and the positions are focused at $r = 3.0$. Their monomer distribution percentages are $P_0 = 65\%$, 76%, and 97%, respectively. This result shows that, the larger the chain stiffness is, the more monomers cling to the cylinder channel.

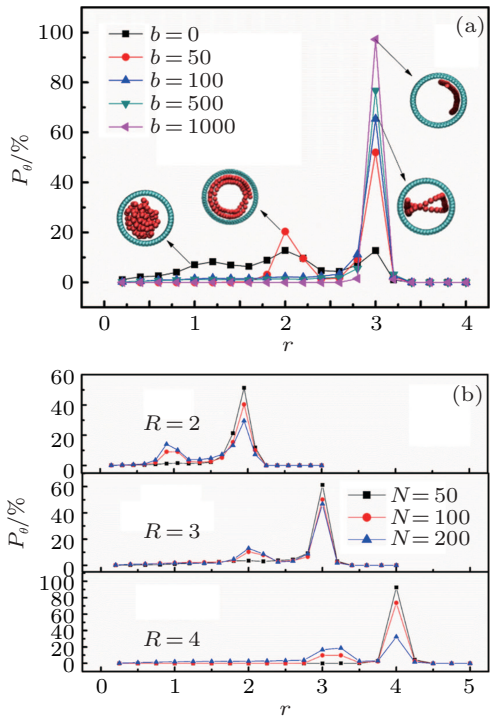


Fig. 7. (color online) (a) Distribution of the polymer monomer along the radial direction of the cylinder channel with identical action radius $R = 3$, monomer number $N = 100$, but with different chain stiffness parameter b. (b) Results with identical chain stiffness parameter $b = 200$, but with different cylinder radius $R = 2$, 3, and 4 from the top to the bottom. Each plot has three curves corresponding to three different chain monomer numbers $N = 50$, 100, and 200, respectively.

Figure 7(b) shows the results of the monomer distribution with identical chain stiffness $b = 200$, and from top to bottom, they represent various conditions with different radius $R = 2$, 3, and 4, respectively. For the curve of $N = 50$ in each plot, there is only one peak. It implies that the monomers all cling to the cylinder channel due to the chain's short length. While $N = 100$ and 200, the corresponding two curves in each plot have two peaks, and the distance between the two peaks approaches 1.0, which has the same mechanism as discussed above in Fig. 7(a). Here it can be seen that, with the chain length increasing, the left peak becomes sharper, while the right peak becomes lower. It is because the longer the chain length is, the larger ratio for the chain to form overlapped helix-like structure, and the two peaks are considered to obey a counter-balanced relation.

The above illustrations are all simulated under the same solution with density $\rho = 0.85$. Actually, we also conduct statistics about other densities. Figure 8(a) illustrates the percentages P_{helix} of helix-like formation with various solution density ρ under identical parameters $R = 3$, $N = 100$, and $b = 200$. It could be seen that when $\rho = 0.85$, the helix percentage is $P_{\text{helix}} = 35\%$, which is the highest percentage compared with the others. Figure 8(b) illustrates the variation of P_{helix} with various chain stiffness b under identical parameters $\rho = 0.85$, $R = 3$, and $N = 100$. Obviously, when $b = 80 \sim 100$, P_{helix} has the highest values 80%, which is the reason why we choose $\rho = 0.85$ as the solution density in the above simulation. From these statistical results, the helix formation percentages vary under different conditions, and there is a peak value at moderate solution particle density and moderate chain stiffness.

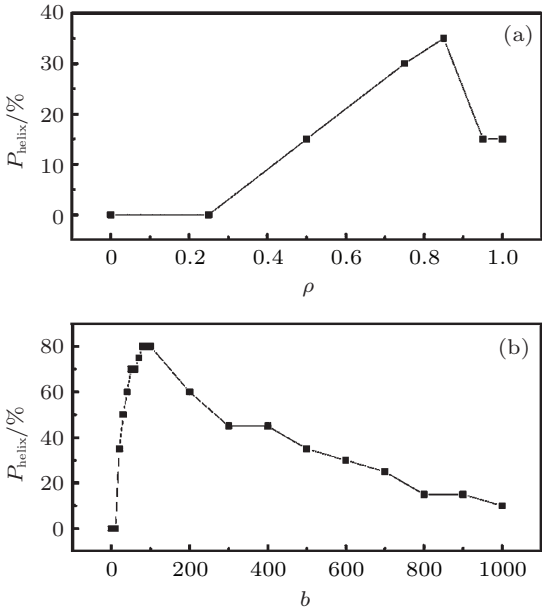


Fig. 8. (a) Helix formation percentages P_{helix} with various solution densities ρ under identical $R = 3$, $N = 100$, and $b = 200$. (b) Helix formation percentages P_{helix} with various chain stiffnesses b under the same $\rho = 0.85$, $R = 3$, and $N = 100$.

4. Conclusions

We have studied the conformation behavior of a semi-flexible polymer chain confined in a cylinder channel, filled with solvent. A novel helix-like structure is found during the simulation which is not a perfect helix structure, but a bundle of turns stuck together. The cross section of the helix structure is not circle, but ellipsoid, whose normal direction is not along the axis direction, but has an included angle from the axis. Moreover, the detailed characteristic parameters such as spatial correlation function and bond angle are calculated to verify the results. In addition, we conduct a statistical analysis for the chain monomer distribution along the radial direction, and find most of the monomers cling to the cylinder channel, except some overlapped situations. The statistical results of the helix formation percentages under various solution density and chain stiffness show that, at moderate solution density and moderate chain stiffness, there is a peak value to form the helix structure. Our work may strengthen the understanding of the microscopic conformations of confined polymer chains under solvent environment.

References

[1] Jeong J, Kang L, Davidson Z S, Collings P J, Lubensky T C and Yodh A G 2015 *Proc. Natl. Acad. Sci. USA* **112** E1837
[2] Dai L, Renner C B and Doyle P S 2015 *Macromolecules* **48** 2812
[3] Azari A and Müller-Nedebock K K 2015 *Europhys. Lett.* **110** 68004
[4] Muralidhar A, Tree D R and Dorfman K D 2014 *Macromolecules* **47** 8446
[5] Maritan A, Micheletti C, Trovato A and Banavar J R 2000 *Nature* **406** 287
[6] Xue B, Wang J and Wang W 2004 *Int. J. Mod. Phys. B* **18** 2123
[7] Wang W, Xu W X, Levy Y, Trizac E and Wolynes P G 2009 *Proc. Natl. Acad. Sci. USA* **106** 5517
[8] Persson F, Utko P, Reisner W, Larsen N B and Kristensen A 2009 *Nano Lett.* **9** 1382
[9] Douville N, Huh D and Takayama S 2008 *Anal. Bioanal. Chem.* **391** 2395
[10] Jo K, Dhingra D M, Odijk T, de Pablo J J, Graham M D, Runnheim R, Forrest D and Schwartz D C 2007 *Proc. Natl. Acad. Sci. USA* **104** 2673
[11] Choi M C, Santangelo C D, Pelletier O, Kim J H, Kwon S Y, Wen Z, Li Y, Pincus P A, Safinya C R and Kim M W 2005 *Macromolecules* **38** 9882
[12] Kasianowicz J J, Brandin E, Branton D and Deamer D W 1996 *Proc. Natl. Acad. Sci. USA* **93** 13770
[13] Reisner W, Pedersen J N and Austin R H 2012 *Rep. Prog. Phys.* **75** 106601
[14] Xu J and Jiang W 2014 *Macromolecules* **47** 2396
[15] Emanuel M 2013 *J. Chem. Phys.* **138** 034903
[16] Dai L, Tree D R, van der Maarel J R C, Dorfman K D and Doyle P S 2013 *Phys. Rev. Lett.* **110** 168105
[17] Tree D R, Wang Y and Dorfman K D 2012 *Phys. Rev. Lett.* **108** 228105
[18] Odijk T 2008 *Phys. Rev. E* **77** 060901
[19] Odijk T 2006 *J. Chem. Phys.* **125** 204904
[20] Lamura A, Burkhardt T W and Gompper G 2004 *Phys. Rev. E* **70** 051804
[21] Burkhardt T W 1997 *J. Phys. A-Math. Gen.* **30** L167
[22] Tree D R, Wang Y and Dorfman K D 2013 *Phys. Rev. Lett.* **110** 208103
[23] Muralidhar A, Tree D R, Wang Y and Dorfman K D 2014 *J. Chem. Phys.* **140** 084905
[24] Liu M, Li W and Qiu F 2013 *J. Chem. Phys.* **138** 104904
[25] Lv C, Xue Q, Shan M, Jing N, Ling C, Zhou X, Jiao Z, Xing W and Yan Z 2013 *Nanoscale* **5** 4191

[26] Wen X, Zhang D and Zhang L 2012 *Polymer* **53** 873
[27] Cifra P and Bleha T 2012 *Soft Matter* **8** 9022
[28] Benková Z and Cifra P 2012 *Macromolecules* **45** 2597
[29] Yang Z, Zhang D, Zhang L, Chen H, Ateeq ur R and Liang H 2011 *Soft Matter* **7** 6836
[30] Witz G, Rechendorff K, Adamcik J and Dietler G 2011 *Phys. Rev. Lett.* **106** 248301
[31] Wang Y, Tree D R and Dorfman K D 2011 *Macromolecules* **44** 6594
[32] Cifra P, Benkova Z and Bleha T 2010 *Phys. Chem. Chem. Phys.* **12** 8935
[33] Cifra P 2009 *J. Chem. Phys.* **131** 224903
[34] Tung W S, Composto R J, Riggleman R A and Winey K I 2015 *Macromolecules* **48** 2324
[35] Wu C 2010 *Polymer* **51** 4452
[36] Dahirel V, Jardat M, Dufrêche J F and Turq P 2007 *J. Chem. Phys.* **126** 114108
[37] Malevanets A and Kapral R 2000 *J. Chem. Phys.* **112** 7260
[38] Plimpton S 1995 *J. Comput. Phys.* **117** 1
[39] Chen Y, Zhang Q and Ding J 2006 *J. Chem. Phys.* **124** 184903
[40] Yasuda S, Yoshidome T, Oshima H, Kodama R, Harano Y and Kinoshita M 2010 *J. Chem. Phys.* **132** 065105
[41] Snir Y and Kamien R D 2007 *Phys. Rev. E* **75** 051114
[42] Snir Y and Kamien R D 2005 *Science* **307** 1067
[43] Magee J E, Vasquez V R and Lue L 2006 *Phys. Rev. Lett.* **96** 207802